ELSEVIER

Biophysical Chemistry 56 (1995) 281–296

Biophysical Chemistry

Conformational studies of the (+)-*trans*, (−)-*trans*, (+)-*cis*, and (−)-*cis* adducts of anti-benzo[*a*]pyrene diolepoxide to N^2-dG in duplex oligonucleotides using polyacrylamide gel electrophoresis and low-temperature fluorescence spectroscopy

Myungkoo Suh [a], Freek Ariese [b], Gerald J. Small [a,b], Ryszard Jankowiak [a,*], Tong-Ming Liu [c], Nicholas E. Geacintov [c]

[a] *Ames Laboratory-USDOE, Ames, IA 50011, USA*
[b] *Department of Chemistry, Iowa State University, Ames, IA 50011, USA*
[c] *Department of Chemistry, New York University, New York, NY 10003, USA*

Received 4 January 1995; accepted 16 March 1995

Abstract

Using polyacrylamide gel electrophoresis (PAGE) and low-temperature, laser-induced fluorescence line narrowing (FLN) and non-line narrowing (NLN) spectroscopic methods, the conformational characteristics of stereochemically defined and site-specific adducts derived from the binding of 7β,8α-dihydroxy-9α,10α-epoxy-7,8,9,10-tetrahydrobenzo[*a*]pyrene (*anti*-BPDE, a metabolite of the environmental carcinogen benzo[*a*]pyrene), to DNA were studied. The focus of these studies was on the four stereochemically distinct *anti*-BPDE modified duplexes 5′-d(CCATCGCTACC)·(GGTAGCGATGG), where G denotes the lesion site derived from *trans* or *cis* addition of the exocyclic amino group of guanine to the C10 position of either (+) or (−)-*anti*-BPDE. PAGE experiments under non-denaturing conditions showed that the (+)-*trans* adduct causes a significantly greater retardation in the electrophoretic mobility than the other three adducts, probably the result of important adduct-induced distortions of the duplex structure. Low-temperature fluorescence studies in frozen aqueous buffer matrices showed that the (+)-*trans* adduct adopts primarily an external conformation with only minor interactions with the helix, but a smaller fraction (~25%) appears to exists in a partially base-stacked conformation. The (−)-*trans* adduct exists almost exclusively (~97%) in an external conformation. Both *cis* adducts were found to be intercalated; strong electron–phonon coupling observed in their FLN spectra provided additional evidence for significant $\pi-\pi$ stacking interactions between the pyrenyl residues and the bases. FLN spectroscopy is shown to be suitable for distinguishing between *trans* and *cis* adducts, but lesions with either (+)- or (−)-*trans*, or (+)- or (−)-*cis* stereochemical characteristics showed very similar vibrational patterns. Addition of glycerol (50%, v/v) to the matrix caused a partial disruption of the chromophore-base stacking interactions for most adducts, but the (−)-*cis* isomer showed a strong blue-shift and unusual vibrational frequencies. Low-temperature fluorescence spectroscopy techniques are most suitable for distinguishing between different conformational benzo[*a*]pyrene diol epoxide-DNA adduct types; because of the sensitivity of these methods, they may provide important information necessary for an understanding of the biological effects of the stereochemically distinct BPDE–guanine lesions.

* Corresponding author.

SSDI 0301-4622(95)00055-0

Keywords: Benzo[*a*]pyrene; BPDE adducts; Polyacrylamide gel electrophoresis; Fluorescence spectroscopy

1. Introduction

Benzo[*a*]pyrene is one of the most intensively studied environmental carcinogens [1,2]. Several enzymatic pathways have been reported to catalyze the binding of this compound or its metabolites to DNA, including monooxygenation [3] and one-electron oxidation routes [4]. Stable DNA adducts are mainly formed via covalent binding of the exocyclic amino group of guanine or adenine to the biologically most active and chemically reactive metabolic intermediate 7,8-dihydroxy-9,10-epoxy-7,8,9,10-tetrahydrobenzo[*a*]pyrene [5]. There are two diastereomeric forms of this molecule, 7β,8α-dihydroxy-9α,10α-epoxy-7,8,9,10-tetrahydrobenzo[*a*]pyrene (*anti*-BPDE), and the 7β,8α,9β,10β-stereoisomer (*syn*-BPDE). Each of these diastereomers can be resolved into (+) and (−) enantiomers, and each enantiomer can react via *cis* or *trans* addition at the C10 position with the exocyclic amino groups of guanine and adenine residues [6,7]. In mammalian cells, racemic (±)-*anti*-BPDE is more mutagenic than (±)-*syn*-BPDE [8,9]. Furthermore, (+)-*anti*-BPDE is strongly tumorigenic while (−)-*anti*-BPDE is not [10,11]. These differences in biological activity are believed to be related to different conformations of the carcinogen DNA adducts [12]. BPDE adducts may adopt various conformations depending on the stereochemistry of the adduct [13] and also depending on the nature of the flanking bases [14,15].

BPDE–DNA adduct conformations have been studied by several techniques, including circular/linear dichroism [14,16], fluorescence spectroscopy [15,17,18], polyacrylamide gel electrophoresis (PAGE) [19], high resolution NMR methods [20], and molecular modelling [21]. In the case of randomly modified BPDE–DNA adducts, the interpretation of data is complicated whenever (1) racemic (±)-*anti*-BPDE is used, (2) mixtures of *cis* and *trans* adducts are formed, (3) different DNA bases are modified, and (4) the sequence contexts in which the different lesions are embedded are not defined. In order to overcome these difficulties it is necessary to synthesize stereochemically pure BPDE adducts bound to a specific group of a given base in a well defined oligonucleotide sequence. Geacintov and coworkers have developed a direct synthetic approach in which BPDE is reacted with a given single stranded oligonucleotide [13,22]. The resulting mixture of BPDE-modified and unmodified oligonucleotide strands with different bases modified and/or different adduct stereochemistries are separated from one another by means of HPLC techniques, and annealed with the complementary strand. This approach was recently used for studying the effects of flanking bases on the characteristics of (+)-*trans*-*anti*-BPDE-N^2-dG adducts [15,23]. For our present study in which conformational differences are investigated as a function of adduct stereochemistry, the same approach was used to synthesize the oligonucleotide d(CCATCGCTACC)·(GGTAGCGATGG) containing the (+)-*trans*, (−)-*trans*, (+)-*cis*, and (−)-*cis* adducts of *anti*-BPDE bound to the exocyclic amino group of the central dG. The chemical structures of the four adducts are presented in Fig. 1. The solution conformations of three of these adducts, bound to the same duplex oligonucleotide, have recently been established by high resolution NMR and molecular mechanics modeling techniques. It was found that the (+)-*trans* and (−)-*trans* adducts are both located in the minor groove, but point in opposite directions (towards the 3′ and 5′ end of the modified strand, respectively) [20,24]. The (+)-*cis* adduct, on the other hand, was found to be characterized by a base-displacement intercalation model, in which the pyrenyl residue is intercalated, while the modified guanine residue and the cytidine residue on the partner strand are displaced into the minor and major grooves, respectively [25].

In this paper we describe conformational studies of these four stereoisomeric BPDE adducts, employing low-temperature laser-induced fluorescence spectroscopy under line narrowing (FLN) and non-line narrowing (NLN) conditions [26], as well as polyacrylamide gel electrophoresis [19]. The determination of BPDE–DNA adduct conformations by NMR techniques requires milligram quantities of purified BPDE-modified oligonucleotides. Fluorescence techniques on the other hand are very sensitive and subnanogram quantities of adducts are often suffi-

cient for identification of the types of adducts [4,26] or their conformational characteristics [15,18,19,27,28]. In addition, fluorescence techniques are capable of distinguishing conformational equilibria on nanosecond and submicrosecond time scales. By comparing results obtained for identical BPDE-modified oligonucleotide duplexes obtained by NMR and by fluorescence methods, more exact interpretations of the lower resolution but higher sensitivity optical spectroscopic techniques such as UV absorbance [29] and fluorescence (this work) become feasible.

2. Materials and methods

2.1. Preparation of the stereospecifically pure adducted oligonucleotides

Racemic *anti*-BPDE was purchased from the National Cancer Institute Chemical Carcinogen Reference Standard Repository (Chemsyn, Inc.), Lot no. CSL-91-320-29-17A, batch 15. The synthesis of the covalent *trans* adducts bound to the d(CCATCGCTACC) sequence at dG was carried out starting from racemic *anti*-BPDE using previously described methods [13,22,30]. Briefly, the stereochemically different 11-mer oligonucleotide adducts were separated and purified by reverse phase HPLC methods. The stereochemical characteristics of the adducts were ascertained by enzymatically digesting the BPDE-modified oligonucleotides to the BPDE-dG mononucleoside levels, and comparing their HPLC retention times and CD spectra with those of (+)-*trans*-, (−)-*trans*-, (+)-*cis*-, and (−)-*cis*-*anti*-BPDE-N^2-dG adduct standards as described by Cheng et al. [7]. The stereochemically pure BPDE-modified oligonucleotide strands 5′-d(CCATCGCTACC) were mixed with equimolar amounts of the complementary strands 5′-d(GGTAGCGATGG), heated to 65°C, and slowly cooled to room temperature. The melting points, T_m, of the duplexes are above 40°C; typical melting profiles have been published [29].

For low-temperature spectroscopic measurements, samples in aqueous buffer (20 mM sodium phosphate, 0.1 M NaCl, pH 7.0) or 50:50 mixed with glycerol, were transferred to 30 μl quartz sample tubes, sealed with rubber septa, and stored at −20°C until further use. Adduct concentrations of all samples were 4×10^{-6} M in aqueous buffer or 2×10^{-6} M in 50% glycerol.

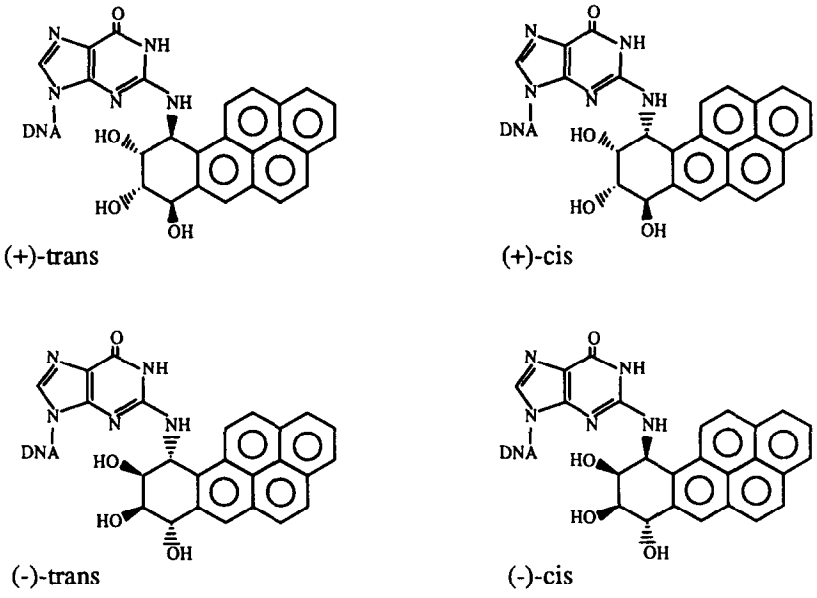

Fig. 1. Stereochemical configurations of the four isomeric adducts of *anti*-BPDE.

2.2. Low-temperature fluorescence measurements

The instrumentation used for low-temperature laser-excited fluorescence spectroscopy has been described elsewhere [26]. Here, only the most important specifications of the apparatus are summarized. The excitation source was a Lambda Physik EMG 103 MSC XeCl excimer laser/FL-2002 dye laser system. Adduct samples were probed with the laser under non-line-narrowing conditions (77 K, $S_2 \leftarrow S_0$ excitation) or line-narrowing conditions (4.2 K, $S_1 \leftarrow S_0$ excitation). Fluorescence was dispersed by a McPherson 2061 1-m monochromator; for NLN measurements the resolution was 0.6 nm (100 μm slit and 150 G/mm grating), while FLN spectra were recorded using a resolution of 0.08 nm (200 μm slit and 2400 G/mm grating). Depending on the grating used the spectral window covered by the active part of the Princeton Instruments IRY-1024/GRB intensified photodiode array detector was 160 nm, or 8 nm, respectively. For gated detection the output of a reference photodiode was used to trigger a Princeton Instruments FG-100 high-voltage pulse generator. Most spectra were recorded using a 45 ns delay and a 400 ns gate width. Before the measurements, samples were thawed from −20°C to room temperature, then first slowly cooled on ice before rapid cooling by the cryogenic liquid. This procedure had previously been found to yield maximum duplexation [15].

2.3. Polyacrylamide gel electrophoresis

The oligonucleotide-BPDE adducts, complementary strands, and unmodified oligonucleotides (controls) were labeled separately with [γ-^{32}P]ATP (New England Nuclear) using T4 polynucleotide kinase from Sigma Inc. Labeling was terminated by incubation at 80°C for 25 minutes. Electrophoresis of duplex oligomers was carried out in two ways: labeled oligonucleotide-BPDE adducts were annealed to the corresponding unlabeled complementary strand, while labeled complementary oligonucleotides were annealed to non-labeled adducted oligonucleotides. In both cases the non-labeled strands were in slight molar excess. Annealing solutions were cooled down from 70°C to 4°C over 2 h and kept at 4°C for an additional 20 minutes, then dried under vacuum in a Speed Vac concentrator. The dried pellets were resuspended in loading buffer (pH 8.3) containing 9 mM tris–borate, 0.2 mM Na_2EDTA, xylene cyanole FF tracking dye (Sigma), and 30% glycerol (v/v).

20% native polyacrylamide gel (19:1 acrylamide:bis-acrylamide in 53 mM tris–borate, 1.2 mM Na_2EDTA, 50 mM NaCl, pH = 8.3 buffer solution) was prepared for the 38 cm × 50 cm Bio-Rad Sequi-Gen Nucleic Acids Sequencing system. Thickness was 0.4 mm. The gel was polymerized at ambient temperature, then placed in a cold room (4°C) and incubated in the running buffer overnight before electrophoresis. Separation was carried out for 60 hours at 320 V and ~ 15 mA. The gel was kept at 4 ± 1°C in the cold room throughout the separation. Autoradiography of gels using various exposure times was done at ambient temperature using Kodak X-ray films.

3. Results and discussion

3.1. PAGE analysis of modified oligonucleotide structures

The autoradiogram in Fig. 2 demonstrates that the PAGE separation of single stranded oligonucleotide samples was excellent, and therefore could be used as an independent purity check. No cross-contamination was observed for the (+)-*trans*, (+)-*cis*, and (−)-*cis* adducts; overexposure revealed only a very low level of contamination (< 0.1%) in the (−)-*trans* sample. Adduct decomposition by hydrolysis would produce a benzo[*a*]pyrene tetrol and the unmodified oligonucleotide, but this was not observed for any of the samples.

In single stranded form, all modified strands move significantly slower than the unmodified control. The retardation of the BPDE-modified oligonucleotides was in the order (+)-*trans*- > (−)-*trans*- > (+)-*cis*- > (−)-*cis*-*anti*-BPDE adduct (see Fig. 2; lanes 1, 2, 3 and 4, respectively). Similar results, but with less pronounced differences in mobilities, were obtained by Shibutani et al. [30] for the same adducts embedded in an 18-mer oligonucleotide. The mobilities must reflect different translational friction coefficients since molecular weight and charge are the same for each adducted strand. However, adduct

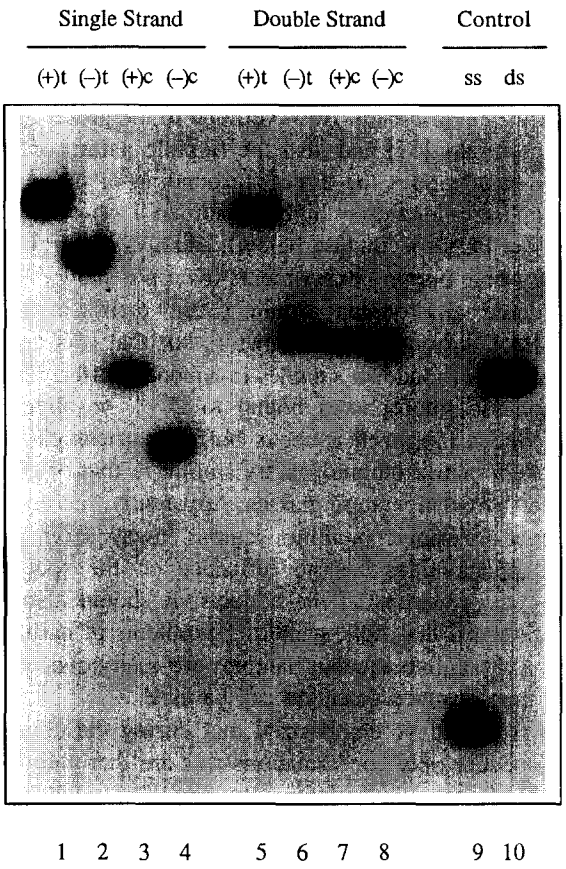

Fig. 2. Autoradiogram showing electrophoretic mobilities (migration direction downwards) of single strand (lanes 1 through 4) and duplex (lanes 5 through 8) oligonucleotides modified by (+)-*trans* (lanes 1 and 5), (−)-*trans* (lanes 2 and 6), (+)-*cis* (lanes 3 and 7), and (−)-*cis* (lanes 4 and 8) adducts of *anti*-BPDE. Lanes 9 and 10 represent the single stranded and duplex unmodified controls, respectively. Conditions: $T = 4°C$, native 20% polyacrylamide slab gel, 50 mM NaCl, 0.6×TBE buffer.

conformations in single stranded oligonucleotides are not the focus of this paper.

In the case of double stranded modified oligonucleotides, the same mobilities were observed independent of whether the modified strand or the complement strand was labeled (only the mobilities of the former are shown in Fig. 2). This indicates that under our experimental conditions (native gel, $T = 4°C$) the modified 11-mer oligonucleotides were in complete duplex form, in agreement with the thermal melting studies of Ya et al. [29]. As shown in Fig. 2, the (−)-*trans*-, (+)-*cis*- and (−)-*cis*-*anti*-BPDE adducted duplexes (lanes 6, 7 and 8, respectively) move slightly slower than the unmodified duplex (lane 10). Considering the molecular weight increase (5%) by adduct formation, these three adducts show minimal deviation in mobility from the duplex unmodified oligonucleotide. On the other hand, the mobility of the (+)-*trans* adduct (lane 5) was drastically reduced. According to the NMR studies of Cosman et al. [20] and de los Santos et al. [24], the extent of solvent exposure of the (+)-*trans*- and (−)-*trans*-*anti*-BPDE adducts are comparable; for both adducts the aromatic moiety is located in the minor groove with one side exposed to the solvent. On the other hand, for the (+)-*cis* adduct (and also for the (−)-*cis* adduct as will be shown below) the pyrenyl system is embedded within the double helix. Thus, there seems to be no clear correlation between the observed gel mobilities and the external/internal character of the adduct. If the observed mobilities of the double stranded modified oligonucleotides are not governed by adduct–solvent interactions, then they must be the result of different adduct-induced distortions of the duplex structure. Several experimental findings indicate bending of the helix at the site of the (+)-*trans*-*anti*-BPDE adduct. Linear dichroism studies of BPDE–DNA adducts with external character, which is characteristic for the (+)-*trans*-*anti*-BPDE adducts, suggested that there is a kink or flexible joint at the site of lesion [31,32]. It was also reported that DNA (145–185 base pairs) modified with (+)-*anti*-BPDE showed reduced electrophoretic mobility, and bending of the helix was suggested [33]. In addition, theoretical molecular dynamics simulation studies reported that the (+)-*trans*-*anti*-BPDE adduct produced severe helical bending in a duplex dodecamer, while the (−)-*trans*-*anti*-BPDE adduct caused only minimal distortion [21]. Our PAGE results confirm those findings, showing that the (+)-*trans*-*anti*-BPDE adduct causes indeed a severe distortion of the overall helix structure, but that the helical structures of the duplex oligonucleotides modified with (−)-*trans*-, (+)-*cis*- or (−)-*cis*-*anti*-BPDE are minimally disturbed. These results are also consistent with those of Mao [34] and Xu et al. [35] who have shown that upon ligation of BPDE-modified oligonucleotides 11–23 base pairs long, only the (+)-*trans*-*anti*-BPDE-modified oligonucleotides are capable of forming small, cova-

lently closed minicircles. This clearly indicates that only the (+)-*trans-anti*-BPDE N^2-dG lesions are associated with a flexible hinge joint or bend at the site of the lesion.

3.2. General remarks concerning low-temperature matrices

Before we discuss the NLN and FLN spectra of the different adduct stereoisomers a short discussion of low-temperature fluorescence measurements and the matrices used in our experiments is appropriate. Compared to conventional fluorescence spectrometry at room temperature, carrying out the measurements at 77 K under non-line narrowing conditions offers several advantages for these types of adducts. Reduced spectral broadening is important in order to observe the sometimes subtle differences in fluorescence spectra. Furthermore, quenching phenomena, affecting the fluorescence of intercalated adducts less strongly than that of external adducts [13,16,17], play only a minor role at cryogenic temperatures; all adduct types exhibit comparable fluorescence lifetimes (ranging from 150 to 200 ns). Apart from the obvious increase in signal intensity, this also means that when non-selective excitation is applied to a mixture of different conformations all adduct types can be observed with similar sensitivities. The relative intensities of different emission bands thus give a direct indication of the relative concentrations of the particular species.

All samples were studied in two matrices: aqueous buffer and aqueous buffer/glycerol 50:50 v/v ('glass'). Obviously the conformations encountered in aqueous buffer mimic the situation in a cellular environment most closely. The addition of glycerol serves several purposes: it increases the solvent compatibility towards the aromatic moiety of the adduct and has a destabilizing effect on the DNA structure. Conformational changes induced by the addition of glycerol thus provide qualitative information regarding the stability of the adduct conformation in aqueous buffer. At the same time the decrease in base-chromophore interactions (weaker electron–phonon coupling) usually leads to better resolved FLN spectra [18], which is useful if the frequencies of the vibrational modes are to be used for identification purposes [4,19,36].

An important question is whether fluorescence line-narrowing spectroscopy is also applicable to frozen aqueous samples that could lead to a crystalline environment. However, due to the presence of buffer salts [37] and also the flexible nature of the oligonucleotides the direct surrounding of the chromophore moieties is highly disordered, as reflected in our FLN spectra (see below), and also our preliminary hole burning experiments (data not shown). An ordered environment could cause matrix-induced (Shpol'skii-type) line-narrowing, but that was never observed for adduct samples in aqueous buffer. Thus, aromatic fluorophores bound to DNA or oligonucleotides in frozen aqueous buffer matrices experience a matrix inhomogeneity similar to that of common low-temperature glasses. Apparently, the occurrence of polycrystalline regions away from the oligonucleotides has no influence on the spectroscopic properties of the adducts. It should also be mentioned that light scattering problems in partially polycrystalline aqueous samples are easily overcome if time-resolved detection can be used.

It should be emphasized that during the cooling procedure only conformations that are thermally accessible at ambient temperature can be trapped. At elevated temperatures the adducts will show a broad distribution of conformations, and some higher-energy conformations may not be trapped during cooling. However, the conformations corresponding to an absolute or local minimum of the potential energy surface will also exist at cryogenic temperatures. Therefore, if two or more distinct molecular conformations are observed in a low-temperature fluorescence experiment, it can be concluded that these conformations do contribute to the conformational equilibrium in solution at biological temperatures, but they may not represent the full room temperature distribution. Since the matrix in the immediate vicinity of the adduct is of an amorphous nature, the possibility that otherwise improbable conformations are being induced by matrix crystallization can be excluded.

3.3. Non-line-narrowing ($S_2 \leftarrow S_0$) fluorescence spectroscopy

In this section non-line narrowed (NLN) fluorescence spectra will be shown for BPDE adducts bound

Table 1
Spectral characteristics of the *anti*-BPDE adduct conformations

	(+)-*trans*			(−)-*trans*			(+)-*cis*			(−)-*cis*		
	Conform. type abundance [c]	(0,0) [a]	Γ [b]	Conform. type abundance	(0,0)	Γ	Conform. type abundance	(0,0)	Γ	Conform. type abundance	(0,0)	Γ
Oligonucleotides in aqueous buffer	(+)-1, major (~ 75%)	378.4	180	(−)-1, major (~ 97%)	378.4	170	(+)-1, minor (~ 6%)	~ 378		(−)-1, minor (~ 8%)	378.5	
	(+)-2, minor (~ 25%)	380.3	~ 240	(−)-2, minor (~ 3%)	380.4	~ 300	(+)-3, major (~ 94%)	381.0	300	(−)-3, major (~ 92%)	381.3	270
Oligonucleotides in 50% glycerol	(+)-1	378.2	200	(−)-1	377.8	200	(+)-1, minor (~ 12%)	377.8	230	(−)-1 [d], minor (~ 15%)	375.7	160
							(+)-3, major (~ 88%)	381.4	330	(−)-3, major (~ 85%)	381.1	300
Mononucleosides in aqueous buffer		376.3	130		376.3	130		376.3	130		376.3	130
Mononucleosides in 50% glycerol		376.5	150		376.5	150		376.5	160		376.5	160

[a] Maximum of fluorescence (0,0) origin band after deconvolution (in nm).
[b] Γ is the FWHM obtained by doubling the half width at half maximum measured at the high energy side of the band (in cm^{-1}).
[c] Relative abundances are estimates obtained upon deconvolution of non-selectively excited NLN spectra.
[d] For this adduct the conformation of the saturated ring is believed to have undergone an important change (see text).

to double stranded oligonucleotides or to deoxyguanosine only. Based on the extent of the red-shift of the fluorescence origin band, we define three different adduct conformations as (±)-1, (±)-2, and (±)-3 [18,27]. These conformations are characterized by increasing stacking interactions with the bases and decreasing accessibility to quenchers, and are assigned as external, partially base stacked, and intercalated adduct types, respectively [18,27]. Most NLN spectra were obtained using excitation at 308 or 343 nm, wavelengths with poor selectivity that one can use to excite external, partially base stacked, and intercalated conformations at the same time with roughly comparable efficiencies (at cryogenic temperatures all adduct types exhibit similar fluorescence lifetimes, while the molar extinction coefficients are not significantly different). Excitation at 355 nm is used to selectively excite intercalated adducts [13]. Selective excitation of external adducts is not possible; the existence of such conformations can only be inferred via spectral deconvolution (see below).

(+)-trans-anti-BPDE adduct

NLN fluorescence spectra obtained for the (+)-*trans* isomer in double stranded oligonucleotide, as well as bound to the nucleoside dG only, are shown in Fig. 3. The solvent matrices were aqueous buffer (curves a, b, d) or aqueous buffer/glycerol 50:50 (curve c). For comparison, curve 3d is the NLN spectrum of the (+)-*trans* adduct bound to guanosine only, showing the typical spectral characteristics (emission maximum 376.3 nm, bandwidth ~ 130 cm^{-1} FWHM) of the BPDE adduct in the absence of interaction with the DNA helix. Emission maxima and widths of the (0,0) origin bands of all adduct isomers are listed in Table 1. Spectrum a in Fig. 3 with its relatively broad (0,0) band (~ 350 cm^{-1}) corresponds to a mixture of conformations. The major one with its maximum at 378.6 nm (a moderate red shift compared to the mononucleoside adduct in spectrum 3d) is assigned, based on our previous nomenclature [18,27], as a (+)-1 external conformation. This agrees very well with the data, reported for this adduct in solution by Cosman et al. [20], showing that the pyrenyl moiety is located in the minor groove with one side exposed to the solvent. However, the skewed peak shape of the fluorescence

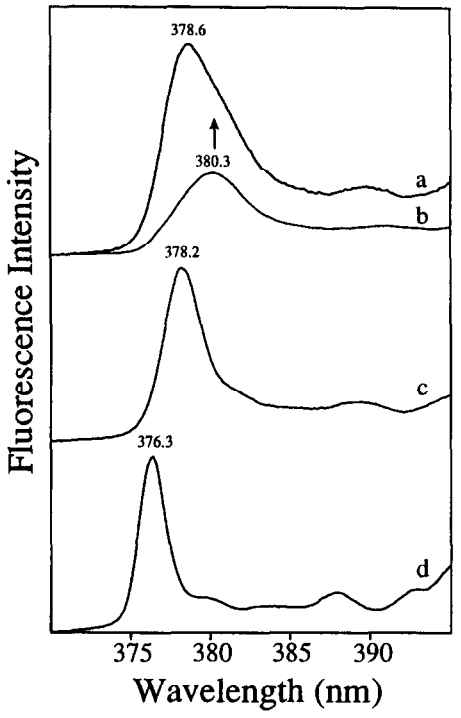

Fig. 3. Non-line narrowed (0,0) fluorescence origin bands of the (+)-*trans*-adduct of *anti*-BPDE in duplex oligonucleotide (T = 77 K) Curve a: spectrum in aqueous buffer; λ_{ex} = 343 nm. Curve b: spectrum in aqueous buffer; λ_{ex} = 355 nm. Curve c: spectrum in 50% glycerol matrix; λ_{ex} = 343 nm. Curve d: spectrum of the same adduct bound to dG only; aqueous buffer; λ_{ex} = 308 nm.

origin band in spectrum 3a indicate that the sample was not conformationally pure, as revealed by selective excitation at 355 nm (see spectrum 3b). This fraction, with its maximum at 380.3 and band width Γ = ~ 240 cm^{-1} is assigned as a (+)-2 type, partially base-stacked conformation; its relative abundance is estimated to be ca. 25% (see Table 1). This is an unexpected finding, since the NMR spectra recorded by Cosman et al. [20] showed no indication of a heterogeneous equilibrium of conformations. The differences in the apparent conformational adduct heterogeneities observed by the fluorescence and high resolution NMR methods are presently not well understood. We note, however, some important experimental differences in these two experiments, for instance, time scales and concentrations. A search for an explanation for these conformational hetero-

geneity effects would have to begin with an investigation of some of these variables, but was beyond the scope of this work.

As observed in previous studies for partially base stacked conformations [38], the addition of glycerol disrupted the weak stacking interactions and the minor (+)-2 contribution observed in aqueous buffer disappeared, leaving a purely external (+)-1 type conformation. This effect is believed to be due to an increased solvent compatibility towards the aromatic moiety. The resulting spectrum, presented in Fig. 3c, is narrower (~ 200 cm^{-1}) and does not show any dependence on the excitation wavelength.

NLN spectra of the single stranded (+)-*trans* adduct sample (not shown) indicates that in aqueous buffer a very broad distribution of external and base-stacked conformations exists (bandwidth ~ 430 cm^{-1}; emission maximum ~ 381 nm). Upon dilution from 4×10^{-6} M to 2×10^{-7} M a significant spectral narrowing and a blue-shift to 376.7 nm is observed. Similar effects were observed upon dilution of the single stranded samples of the (−)-*trans* and (+)-*cis* adducts, but not for the (−)-*cis* adduct. Studies in progress are expected to clarify these phenomena for single stranded oligonucleotides. In this paper we focus only on structural properties of adducts in duplex oligonucleotides.

(−)-trans-anti-BPDE adduct

NLN spectra of the double stranded (−)-*trans* adduct, obtained using non-selective excitation at 343 nm, are shown in Fig. 4, curves a and b. The emission maximum at 378.4 nm observed in aqueous buffer (spectrum 4a) corresponds to a (−)-1 external adduct type with only weak interactions with the DNA helix. The (0,0) origin band of the (−)-*trans* adduct is very narrow (~ 170 cm^{-1}), indicating minimal heterogeneity. Excitation wavelength dependence was practically absent; a very small contribution with a red-shifted emission was observed when 355 nm excitation was employed (spectrum not shown). Addition of glycerol to the sample did not have a large impact on the width of its NLN spectrum (compare spectrum 4b with 4a). However, the (0,0) origin band was found to undergo a 0.6 nm blue-shift, which was not observed for the (+)-*trans* adduct. The bottom curve 4c shows the NLN spectrum of the (−)-*trans* adduct to dG for comparison.

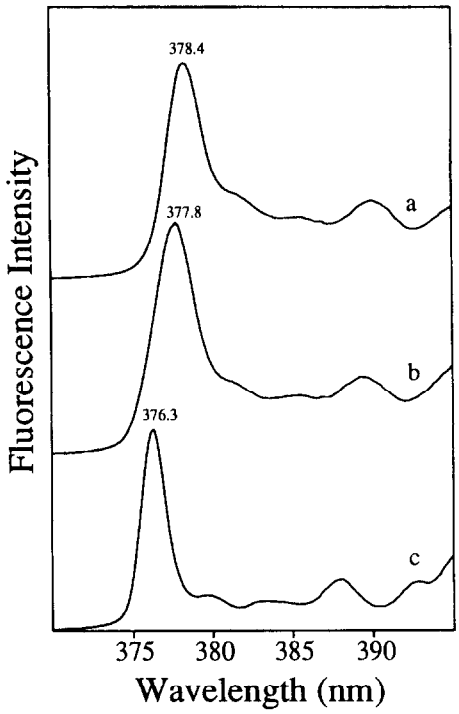

Fig. 4. Non-line narrowed (0,0) fluorescence origin bands of the (−)-*trans*-adduct of *anti*-BPDE in duplex oligonucleotide ($T = 77$ K) Curve a: spectrum in aqueous buffer; $\lambda_{ex} = 343$ nm. Curve b: spectrum in 50% glycerol matrix; $\lambda_{ex} = 343$ nm. Curve c: spectrum of the same adduct bound to dG only; aqueous buffer; $\lambda_{ex} = 308$ nm.

Our conformational assignment as a (−)-1 external adduct is in agreement with the studies of de los Santos et al. [24], who reported that the (−)-*trans* adduct is located in the minor groove with one face of the aromatic moiety exposed to the solvent. The fact that the two *trans* adducts behave differently upon the addition of glycerol indicates that the interactions with the DNA are not identical.

(+)-cis-anti-BPDE adduct

The NLN spectra of the *cis* adduct of (+)-*anti*-BPDE are shown in Fig. 5. In aqueous buffer matrix (spectrum 5a, employing non-selective excitation at 308 nm) the major conformation showed strong chromophore–base interactions: the width is ca. 300 cm^{-1}, while the emission maximum at 381.0 nm is significantly red-shifted compared to those of the

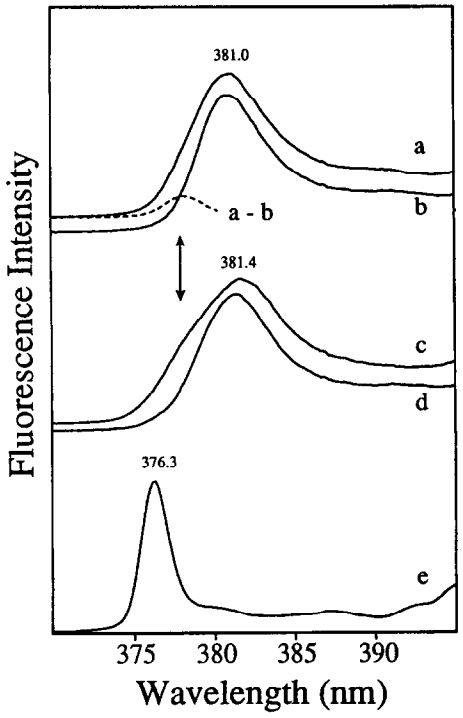

Fig. 5. Non-line narrowed (0,0) fluorescence origin bands of the (+)-*cis*-adduct of *anti*-BPDE in duplex oligonucleotide ($T = 77$ K) Curve a: spectrum in aqueous buffer; $\lambda_{ex} = 308$ nm. Curve b: spectrum in aqueous buffer; $\lambda_{ex} = 355$ nm. Dashed curve: difference spectrum 5a − 5b. Curve c: spectrum in 50% glycerol matrix; $\lambda_{ex} = 308$ nm. Curve d: spectrum in 50% glycerol matrix; $\lambda_{ex} = 355$ nm. Curve e: spectrum of the same adduct bound to dG only; aqueous buffer; $\lambda_{ex} = 308$ nm.

two *trans* adducts discussed above. This indicates that in the duplex oligonucleotide the adduct is held in an internal (+)-3 type conformation. These results agree with the findings of Cosman et al. [25], who recently established the major solution conformation of this adduct to be of the intercalated type, with the pyrenyl moiety being sandwiched between the two neighboring cytidine bases and displacing not only the adducted guanine into the minor groove, but also the opposite cytidine residue on the partner strand into the major groove. When using selective excitation at 355 nm a minor conformational heterogeneity is observed, as can be seen by comparing spectra 5a and 5b. The dashed curve represents the difference spectrum. This minor fraction, with its origin band around 378 nm, is less efficiently excited at 355 nm, indicating that its conformation must be of the external type [13]. Also Cosman et al. [25] noticed the existence of a minor, non-intercalative conformation in their NMR study, in agreement with our findings.

Addition of glycerol to the aqueous sample increases the solvent compatibility towards the aromatic moiety and may also disrupt the helical structure. Both effects can be illustrated in the case of the (+)-*cis* adduct. The very broad origin band of the duplex sample in 50% glycerol indicates a mixture of external and intercalated adducts (see Fig. 5c). The glycerol causes a larger fraction of the adduct molecules to adopt an external conformation (larger shoulder around 378 nm in spectrum 5c than in spectrum 5a). The fact that the major origin band is still at 381.4 nm shows that, unlike the partially base-stacked (+)-2 conformation observed for the (+)-*trans* adduct, the truly intercalated (+)-3 type conformation is relatively stable in this matrix, as was previously demonstrated for these adducts in double stranded oligonucleotides [38] and in DNA [27]. The 30 cm^{-1} increase in spectral bandwidth of the intercalated conformation (compare curves 5d and 5b, both obtained employing selective excitation at 355 nm; see also Table 1) presumably reflects a destabilization of the helical structure in the 50% glycerol matrix, leading to a broader distribution of intercalated structures. Again the bottom curve 5e shows the NLN spectrum of the (+)-*cis*-*anti*-BPDE-dG adduct for comparison.

(−)-*cis*-*anti*-BPDE adduct

NLN spectra of the (−)-*cis* adduct are shown in Fig. 6. The spectrum of the duplex sample in aqueous buffer (curve 6a) is very similar to that of the (+)-*cis* adduct. The (0,0) band is red-shifted to 381.3 nm, which according to our nomenclature corresponds to a (−)-3 type internal adduct conformation [18,27], and almost as broad as that of the (+)-*cis* adduct. For this adduct no independent structure characterization by means of high resolution NMR spectroscopy has yet been published, but based on the similarity between the spectral properties of the two *cis* adducts we conclude that also the (−)-*cis*-*anti*-BPDE adduct adopts an intercalated conformation [13]. Further evidence will be provided in the next section by means of FLN spectroscopy. The sample showed only minor excitation wave-

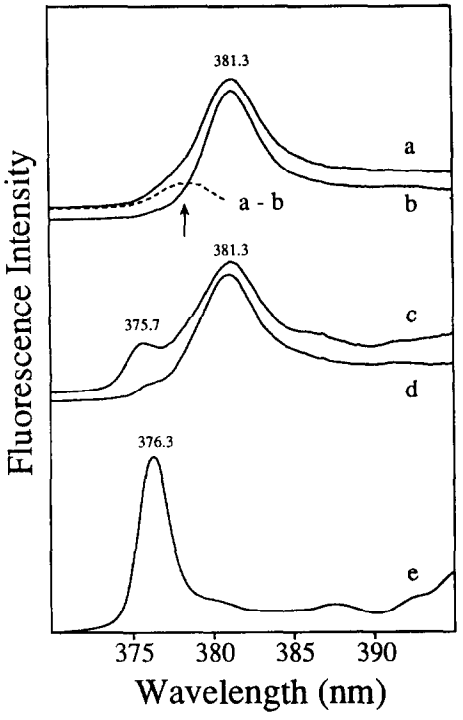

Fig. 6. Non-line narrowed (0,0) fluorescence origin bands of the (−)-*cis*-adduct of *anti*-BPDE in duplex oligonucleotide ($T = 77$ K) Curve a: spectrum in aqueous buffer; $\lambda_{ex} = 308$ nm. Curve b: spectrum in aqueous buffer; $\lambda_{ex} = 355$ nm. Dashed curve: difference spectrum 6a − 6b. Curve c: spectrum in 50% glycerol matrix; $\lambda_{ex} = 308$ nm. Curve d: spectrum in 50% glycerol matrix; $\lambda_{ex} = 355$ nm. Curve e: spectrum of the same adduct bound to dG only; aqueous buffer; $\lambda_{ex} = 308$ nm.

length dependence, as can be seen by comparing curves 6a and 6b. The dashed curve represents the difference spectrum 6a − 6b. As in the case of the (+)-*cis* adduct, a minor contribution (~ 8%) of an adduct with an external conformation can be discerned around 378.5 nm.

In the 50% glycerol matrix the majority of the adduct molecules are still intercalated, which means that also for this adduct the intercalated conformation is relatively stable (see curve 6c). However, an important fraction has adopted a conformation that shows an emission maximum around 375.7 nm, more blue-shifted than observed for the external fractions of the other three adduct samples and even more blue-shifted than the mononucleoside adduct (curve 6e). When 355 nm excitation is used only the intercalated fraction of the conformational mixture is observed (spectrum 6d). More information on the nature of this peculiar conformational equilibrium was obtained using FLN spectroscopy (see below).

Finally, we note that under NLN conditions the spectra of the single nucleoside adducts are very similar for all four stereoisomers (compare the bottom spectra of Fig. 3, Fig. 4, Fig. 5, and Fig. 6), and practically independent of the solvent matrix used (see Table 1). However, *cis* and *trans* isomers are easily distinguished under FLN conditions, as will be shown in the next section.

3.4. Fluorescence line narrowing spectroscopy

More detailed structural information concerning the different BPDE adducts can be obtained using fluorescence line narrowing spectroscopy. In the study of carcinogen DNA adducts this technique may be used to obtain extra conformational information or it can serve chemical/stereochemical identification purposes [26]. Both aspects will now be discussed separately.

In a typical vibronically excited FLN spectrum each S_1 vibrational frequency will appear as a sharp line (the zero-phonon line, ZPL), accompanied by a broader band at longer wavelength. The latter, so-called phonon side band (PSB), is attributed to molecules that lose part of their excitation energy to lattice vibrations (phonons). The ZPL/PSB intensity ratio strongly depends on temperature and the electronic coupling with the matrix, and can thus provide information on the microenvironment around the chromophore. It was shown by Haarer [39] that π-molecular charge-transfer states are characterized by very strong coupling. Jankowiak and coworkers [27] have shown that the relative intensities of the ZPLs in the FLN excitation spectra of various (+)-*anti*-BPDE–DNA adducts increases in the order (+)-3 intercalated < (+)-2 partially base-stacked < (+)-1 external, reflecting a decrease in coupling strength between the chromophore and the bases in the same order.

FLN spectra obtained for the four adduct stereoisomers in double-stranded oligonucleotides in aqueous buffer matrix are shown in Fig. 7. The spectra were recorded at liquid helium temperature (4.2 K) using 369.48 nm excitation; at this wavelength broad-banded emission due to uncorrelated

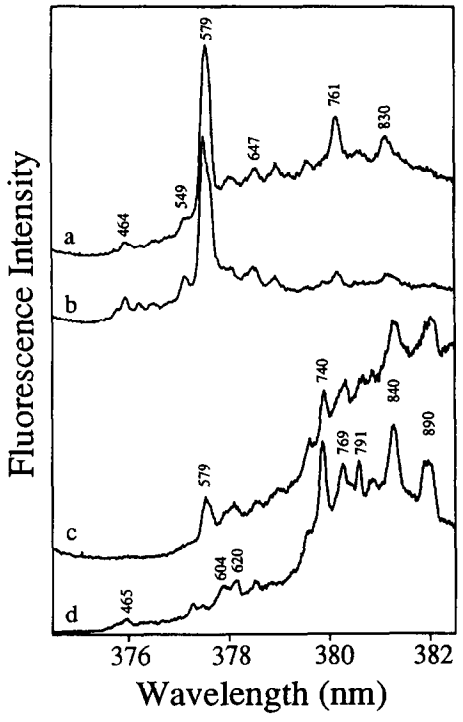

Fig. 7. FLN spectra of the duplex oligonucleotides in aqueous buffer, containing different stereoisomeric *anti*-BPDE-N^2-dG adducts. Curve a: (+)-*trans*; curve b: (−)-*trans*; curve c: (+)-*cis*; curve d: (−)-*cis* adduct. $T = 4.2$ K; $\lambda_{ex} = 369.48$ nm. Zero-phonon lines are labeled with their excited-state vibrational frequencies (in cm^{-1}).

S_2-S_0 excitation can be ruled out. In the 378 nm region the (+)-*trans* adduct yields a fairly well resolved FLN spectrum with strong ZPL's (curve 7a; spectra obtained using other excitation wavelengths not shown). This indicates that there are no strong stacking interactions with the bases. These findings for the major adduct are in full agreement with the solution conformation established for the (+)-*trans* adduct by Cosman et al. [20], in which the pyrenyl moiety is situated in the minor groove, with one side interacting with the sugar-phosphate backbone and one side exposed to the solvent. However, the broad emission band underlying the low-energy side of the spectrum (~ 380 nm) indicates the presence of a second, minor conformation with stronger stacking interactions, in agreement with the NLN results discussed above and shown in Fig. 3, spectra a and b.

In contrast, the FLN spectrum of the (−)-*trans*-*anti* adduct (curve 7b) does not show any broad-banded emission indicative of stacking interactions. This adduct exists in a pure (−)-1 type external conformation. These results are in full agreement with the solution conformation reported by de los Santos et al. [24], in which the adduct is located in the minor groove (pointing towards the 3′ terminus of the modified strand) and interacts only with the solvent and the sugar-phosphate backbone.

Spectrum 7c shows that the FLN spectrum of the (+)-*cis* adduct is distinctly different. The intensities of the ZPLs are relatively weak and superimposed on a strong broad-banded emission at the low-energy side of the spectrum. This proves that the broad (0,0) band around 381 nm observed at 77 K (Fig. 5a) is not due to a broad heterogeneous distribution of adduct conformations, but to strong electron–phonon coupling (π–π interactions). Again, these findings are in full agreement with the intercalated conformation established for this adduct by Cosman et al. [25]. The ZPL's in the 378 nm region belong to the minor external conformation shown in Fig. 5 (difference spectrum 5a − 5b).

Curve 7d shows that the FLN spectrum of the (−)-*cis* adduct is very similar to that of its (+)-*cis* counterpart. The (−)-*cis* adduct shows also relatively weak ZPLs with a large contribution from phonon side bands, indicating that also for this adduct the major conformation, assigned as (−)-3, is one in which the chromophore experiences very strong coupling with the bases. These spectra confirm our conclusion of the previous subsection that also the (−)-*cis* adduct adopts primarily an intercalated conformation. Also for this adduct the ZPL's in the 378 nm region belong to the minor external conformation (see Fig. 6, difference spectrum 6a − 6b).

The FLN spectra obtained in 50% glycerol matrix are presented in Fig. 8 and confirm the NLN results discussed above. In the case of the (+)-*trans* adduct the weak stacking interactions are disrupted, resulting in a purely external (+)-1 type conformation (see spectrum 8a). The spectrum of (−)-*trans*-*anti*-BPDE is blue-shifted by 0.6 nm upon the addition of glycerol, and as a result the low-frequency modes around 376 nm increase in intensity, while the vibronic lines in the 380 nm region decrease (compare spectra 8b and 7b). Such behavior is not observed for the (+)-*trans* isomer. These differences could be

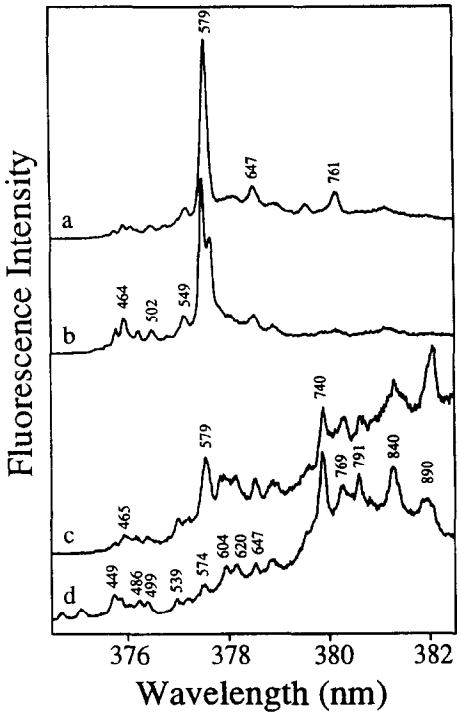

Fig. 8. FLN spectra of the duplex oligonucleotides in 50% glycerol matrix, containing different stereoisomeric *anti*-BPDE-N^2-dG adducts. Curve a: (+)-*trans*; curve b: (−)-*trans*; curve c: (+)-*cis*; curve d: (−)-*cis* adduct. $T = 4.2$ K; $\lambda_{ex} = 369.48$ nm. Zero-phonon lines are labeled with their excited-state vibrational frequencies (in cm^{-1}).

related to the findings of de los Santos et al. [24], who stated that the interactions between the aromatic moiety and the minor groove are not identical for the two *trans* isomers. Fig. 8c illustrates again that for the (+)-*cis* adduct even in 50% glycerol the intercalated structure remains largely intact, but that a minor contribution of an external (+)-1 conformation is also present in this matrix. The relative contribution of this minor fraction is larger in this matrix than in aqueous buffer (compare spectra 8c and 7c). Curve 8d shows the FLN spectrum obtained for the (−)-*cis* adduct. The intercalated conformation remains the major one, but for this adduct, besides the minor external contribution around 378 nm which was also observed in aqueous buffer, the presence of an unknown conformation with an unusually blue-shifted (0,0) band around 376 nm is also observed in this matrix (see below for further details).

When comparing the vibrational frequency patterns of the four adduct stereoisomers in Figs. 7 and 8, it is observed that *trans* and *cis* adducts are very easily distinguished (see also spectra 9b and 9c for the mononucleoside adducts). For example, ZPLs at 549 and 761 cm^{-1} are indicative of *trans* adducts, while strong lines at 539, 740, or 890 cm^{-1} are observed for the *cis* adducts. However, when comparing the vibrational frequencies of the two *trans* spectra there is only a small number of obvious differences (e.g. the 579 cm^{-1} mode) and also for the two *cis* adducts only minor differences were observed (e.g. the 600–620 cm^{-1} region). In the case of the stereoisomeric mononucleosides, (+)-*trans*, (−)-*trans*, (+)-*cis*, and (−)-*cis* adducts yield NLN spectra which are similar in all cases, but the FLN spectra are different for the *trans* and the *cis* adducts. However, (+)- and (−)-*trans* or -*cis* adducts cannot be distinguished from one another (also when different excitation wavelengths were used to explore other regions of the S_1 excited state; spectra not shown). Apparently, the influence of the sugar moiety on the fluorescence characteristics of these stereoisomeric BPDE-mononucleoside adducts is negligible. The major excited state vibrational frequencies are listed in Table 2.

Different interactions with the DNA helix, duplex formation, or solvent effects may change the intensity distribution of the ZPLs or increase the intensity of the broad phonon side bands, but the frequencies remain usually unchanged. One of the exceptions observed for these adducts is the splitting of the 579 band for the (−)-*trans* isomer as shown in Fig. 7b, which is even more pronounced in the 50% glycerol matrix (curve 8b). No splitting was observed in single stranded samples or in the FLN spectra of the (+)-*trans*- and (−)-*trans* mononucleoside adducts. It appears that the splitting must reflect how this particular duplex structure influences the conformation of the (−)-*trans* adduct. However, it should be mentioned that this effect cannot be used in a general way to distinguish (−)-*trans* from (+)-*trans* adducts, since splitting was also observed for the (+)-*trans* isomer in a d(...TGG...)(...CCA...) sequence [15].

Comparison of the spectra of the two *cis* adducts reveals that in aqueous buffer matrix the vibrational frequencies are very similar. Most frequencies also

agree well with those found for the *cis-anti*-BPDE-dG adducts. Only minor differences were observed in the 575–620 cm^{-1} region. Interestingly, in the 50% glycerol matrix only the low-energy part of the two *cis* spectra (curves 8c and 8d) are similar. The blue-shifted fraction of the (−)-*cis* adduct, on the other hand, shows an unusual vibrational pattern, different from that observed in aqueous buffer, different from that of the (+)-*cis* adduct, and also different from that of the free (−)-*cis-anti*-BPDE-dG adduct. The latter is illustrated in Fig. 9, comparing the FLN spectra of the (−)-*cis* adduct in duplex oligonucleotide (curve 9a) and bound to dG only (curve 9b). It is clear that for the (−)-*cis* adduct the addition of glycerol has induced more than just a diminished interaction with the bases. It appears that the effect is caused by a structural change in the saturated ring, having a direct influence on the vibrational properties of the aromatic moiety. Multidimensional NMR studies and/or molecular modelling will be needed to test this hypothesis and to help answering the question why this phenomenon is observed for the (−)-*cis* adduct only.

Table 2
Most prominent excited state vibrational frequencies in FLN spectra of *anti*-BPDE adducts [a]

(+)-*trans*/(−)-*trans*	(+)-*cis*/(−)-*cis*	(−)-*cis* [b]
453	453	449
464	465	461
483	481	486
502	496	499
549	539	539
579(+);575/583(−) [c]	579(+);574(−)	564
	604/620	601/621
647	647	
720	740	719
761	769	755
	791	784
830	840	842
	890	863
957	949	955
1044	1026	1029
1108	1108	1110
1384	1383	1365/1378
1441	1441	1441

[a] Vibrational frequencies are identical for (+) and (−)-*trans*, and for (+) and (−)-*cis* adducts, unless otherwise indicated. Frequencies are given in wave numbers; accuracy ±2 cm^{-1}.
[b] Refers to the blue-shifted component of the (−)-*cis* adduct spectra (only observed in duplex samples in water/glycerol matrix).
[c] Splitting of the 579 cm^{-1} band depends on duplexation, solvent matrix, and DNA sequence (see also text).

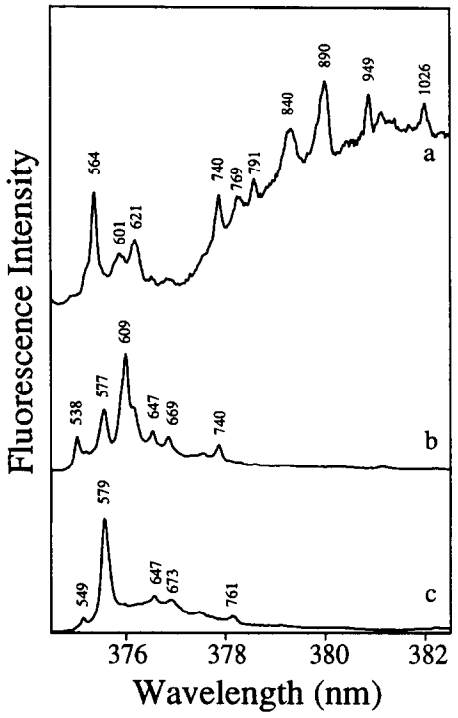

Fig. 9. FLN spectra of *anti*-BPDE adducts in 50% glycerol matrix. Curve a: (−)-*cis* adduct bound to duplex oligonucleotide; curve b: spectrum of the (−)-*cis* adduct bound to dG only; curve c: spectrum of the (−)-*trans* adduct bound to dG only. $T = 4.2$ K, λ_{ex}: 367.58 nm. Zero-phonon lines are labeled with their excited-state vibrational frequencies (in cm^{-1}).

4. Conclusions

The gel electrophoresis experiments of the modified duplex oligonucleotides show that the (+)-*trans* adduct causes a significant retardation, but that the mobility of the other three adducts is similar to that of the unmodified control. On the other hand, the fluorescence data show that the adduct conformation and the extent of solvent exposure are comparable for the two *trans* and for the two *cis* adducts. For adducted oligonucleotides in double stranded form we conclude that PAGE and fluorescence spectroscopy may be regarded as complementary techniques, the former providing more information on

perturbation of the overall helical structure, the latter reflecting the direct environment of the chromophore.

We have demonstrated that using low-temperature fluorescence methods not only major but also minor adduct conformations can be characterized. Compared to room-temperature measurements, e.g. Geacintov et al. [13], the use of cryogenic techniques increases sample stability, reduces spectral broadening, and because of the elimination of quenching processes, all adduct conformations have comparably high fluorescence quantum yields [28]. Another important advantage is that the same techniques can also be employed to study adduct conformations in single stranded oligonucleotides and in whole pieces of intact DNA, in solution or in solid form.

FLN spectroscopy offers additional information on adduct conformations. Based on the extent of electron–phonon coupling one can distinguish between a broad heterogeneous distribution of external, solvent-exposed adducts (as in the case of the (+)-*trans* adduct in aqueous buffer) and a conformation with strong $\pi-\pi$ interactions between the chromophore and its microenvironment (as was found for the intercalated *cis* adducts). Furthermore, the vibrational patterns of the FLN spectra are clearly different, and can be used to distinguish *cis* from *trans* adducts. However, the FLN technique is often of limited value for distinguishing between (+)- and (−)-*trans*, or (+)- and (−)-*cis* adduct configurations. In principle, however, the FLN method may be capable of distinguishing adducts derived from the binding of enantiomeric diol epoxides to DNA; the configurations of the different OH groups and the orientation of the BPDE-N^2 linkage at chiral binding sites may give rise to different degrees of interactions with neighboring bases, and thus to blue or red shifts in the spectra. However, the vibrational frequencies of the chromophore are usually not affected. An interesting exception to this rule was observed in the case of the (−)-*cis* adduct in 50% glycerol.

For the (+)-*trans-anti*-BPDE-N^2-dG adduct, typically the major stable adduct when DNA is exposed to benzo[*a*]pyrene or BPDE [1,3,40], it was found that the adduct mainly exists in a partially solvent-exposed conformation with little stacking interaction with the bases. These results are, of course, in very good agreement with the solution conformation determined for the same adduct by Cosman et al. [20]. However, the sample was not conformationally pure: we also found a minor conformation with a more base-stacked character. The same was observed for the (+)-*trans-anti*-BPDE-N^2-dG adduct in oligonucleotide sequences with a 5′ guanine neighbor [15].

The data obtained for the (−)-*trans* adduct indicate that the extent of solvent exposure is similar to the major conformation of the (+)-*trans* adduct, but in the case of (−)-*trans* there is only minimal conformational heterogeneity. For this adduct the agreement with the NMR/molecular modelling studies of de los Santos et al. [24] is excellent.

In the case of the (+)-*cis* adduct all spectral evidence indicates an intercalated structure for the major conformation, with only a very minor contribution with a more solvent-exposed character. Again, these results are in very good agreement with the solution structure reported by Cosman et al. [25] and with other spectroscopic studies indicating a base-stacked, internal adduct conformation [13].

For the (−)-*cis* adduct no structure based on NMR data has yet been published. Earlier fluorescence data by Geacintov et al. [13] for this adduct (in a –TGT– sequence) showed a strong red-shift, presumably caused by intercalation. The present results, in particular the strong electron–phonon coupling observed in the FLN spectra and the red-shift of the (0,0) origin band, prove that the (−)-*cis* adduct is indeed intercalated.

In conclusion, we would like to stress that fluorescence techniques cannot be expected to provide the same level of structural detail as two-dimensional NMR studies combined with molecular modelling. Fluorescence-based methods, however, are less time-consuming, require orders of magnitude less material, and are applicable to a wider range of samples, especially larger-sized native DNA molecules. At the same time they do provide very useful structural information including insight on adduct conformations and/or conformational equilibria for adducts with different stereochemistries or for adducts in different base sequence contexts [15]. Such conformational studies could provide important clues as to which factors influence the kinds and frequencies of mutations observed as the result of adduct formation [41,42].

Acknowledgements

Ames Laboratory is operated for the U.S. Department of Energy by Iowa State University under contract no. W-7405-Eng-82. This work was supported by the Office of Health and Environmental Research, Office of Energy Research. The portion of the work performed at New York University was supported by the Office of Health and Environmental Research, The Department of Energy, Grant DE-FG02-86ER60405.

References

[1] D.H.Phillips, Nature, 303 (1983) 468–472.
[2] M.R. Osborne and N.T. Crosby, Benzopyrenes, Chapters 1–10, Cambridge University Press, Cambridge, UK, 1987.
[3] A.H. Conney, Cancer Res., 42 (1982) 4875–4917.
[4] E.G. Rogan, P.D. Devanesan, N.V.S. RamaKrishna, S. Higginbotham, N.S. Padmavathi, K. Chapman, E.L. Cavalieri, H. Jeong, R. Jankowiak and G.J. Small, Chem. Res. Toxicol., 6 (1993) 356–363.
[5] E. Huberman, L. Sachs, S.K. Yang and H.V. Gelboin, Proc. Natl. Acad. Sci. USA, 73 (1976) 607–611.
[6] T. Meehan and K. Straub, Nature, 277 (1979) 410–412
[7] S.C. Cheng, B.D. Hilton, J.M. Roman and A. Dipple, Chem. Res. Toxicol., 2 (1989) 334–340.
[8] R.F. Newbold and P. Brookes, Nature, 261 (1976) 52–54.
[9] A.W. Wood, R.L. Chang, W. Levin, H. Yagi, D.R. Thakker, D.M. Jerina and A.H. Conney, Biochem. Biophys. Res. Commun., 77 (1977) 1389–1396.
[10] T.J. Slaga, W.J. Bracken, G. Gleason, W. Levin, H. Yagi, D.M. Jerina and A.H. Conney, Cancer Res., 39 (1979) 67–71.
[11] M.K. Buening, P.G. Wislocki, W. Levin, H. Yagi, D.R. Thakker, H. Akagi, M. Koreeda, D.M. Jerina and A.H. Conney, Proc. Natl. Acad. Sci. USA, 75 (1978) 5358–5361.
[12] P. Brookes and M.R. Osborne, Carcinogenesis, 3 (1982) 1223–1226.
[13] N.E. Geacintov, M. Cosman, B. Mao, A., Alfano, V. Ibanez and R.G. Harvey, Carcinogenesis, 12 (1991) 2099–2108.
[14] C.J. Roche, A.M. Jeffrey, B. Mao, A. Alfano, S.K. Kim, V. Ibanez and N.E. Geacintov, Chem. Res. Toxicol., 4 (1991) 311–317.
[15] M. Suh, R. Jankowiak, F. Ariese, B. Mao, N.E. Geacintov and G.J. Small, Carcinogenesis, 15 (1994) 2891–2898.
[16] A. Gräslund and B. Jernström, Q. Rev. Biophys., 22 (1989) 1–37.
[17] N.E. Geacintov and S.K. Kim, in W.R.G. Baeyens, D. De Keukeleire and K. Korkidis (Editors), Practical Spectroscopy Series, Vol., 12: Luminescence Techniques on Chemical and Biochemical Analysis, Marcel Dekker, New York, 1991, pp. 317–338.
[18] P. Lu, H. Jeong, R. Jankowiak, G.J. Small, S.K. Kim, M. Cosman and N.E. Geacintov, Chem. Res. Toxicol., 4 (1991) 58–69.
[19] G.A. Marsch, R. Jankowiak, M. Suh and G.J. Small, Chem. Res. Toxicol., 7 (1994) 98–109.
[20] M. Cosman, C. de los Santos, R. Fiala, B.E. Hingerty, S.B. Singh, V. Ibanez, L.A. Margulis, D. Live, N.E. Geacintov, S. Broyde and D.J. Patel, Proc. Natl. Acad. Sci. USA, 89 (1992) 1914–1918.
[21] S.B. Singh, B.E. Hingerty, U.C. Singh, J.P. Greenberg, N.E. Geacintov and S. Broyde, Cancer Res., 51 (1991) 3482–3492.
[22] M. Cosman, V. Ibanez, N.E. Geacintov and R.G. Harvey, Carcinogenesis, 11 (1990) 1667–1672.
[23] M. Mao, J. Xu, L. Margulis, S. Smirnov, B. Li, N.Q. Ya and N.E. Geacintov, Carcinogenesis, 16 (1995) 357–365.
[24] C. de los Santos, M. Cosman, B.E. Hingerty, V. Ibanez, L.A. Margulis, N.E. Geacintov, S. Broyde and D.J. Patel, Biochemistry, 31 (1992) 5245–5252.
[25] M. Cosman, C. de los Santos, R. Fiala, B.E. Hingerty, V. Ibanez, E. Luna, R.G. Harvey, N.E. Geacintov, S. Broyde and D.J. Patel, Biochemistry, 32 (1993) 4145–4155.
[26] R. Jankowiak and G.J. Small, Chem. Res. Toxicol., 4 (1991) 256–269.
[27] R. Jankowiak, P. Lu, G.J. Small and N.E. Geacintov, Chem. Res. Toxicol., 3 (1990) 39–46.
[28] R. Zhao, T. Liu, S.K. Kim, M.C. MacLeod and N.E. Geacintov, Carcinogenesis, 13 (1992) 1817–1824.
[29] N.-Q. Ya, S. Smirnov, M. Cosman, S. Bhanot, V. Ibanez and N.E. Geacintov, in R.H. Sarma and M.H. Sarma (Editors), Structural Biology; The State of the Art, Proc. 8th Conversation, Vol. 2, Adenine Press, Schenectady, NY, 1994, pp. 349–366.
[30] S. Shibutani, L.A. Margulis, N.E. Geacintov and A.P. Grollman, Biochemistry, 32 (1993) 7531–7541.
[31] M. Eriksson, B. Nordén, B. Jernström and A. Gräslund, Biochemistry, 27 (1988) 1213–1221.
[32] C.J. Roche, N.E. Geacintov, V. Ibanez and R.G. Harvey, Biophys. Chem., 33 (1989) 277–288.
[33] M.E. Hogan, N. Dattagupta and J.P. Whitlock, Jr., J. Biol. Chem., 256 (1981) 4504–4513.
[34] B. Mao, Ph.D. Thesis, New York University (1993).
[35] R. Xu, B. Mao, J. Xu, B. Li, S. Birke, C.E. Swenberg and N.E. Geacintov, Nucl. Acids Res., (1995) in press.
[36] P.D. Devanesan, N.V.S. RamaKrishna, R. Todorovic, E.G. Rogan, E.L. Cavalieri, H. Jeong, R. Jankowiak, G.J. Small, Chem. Res. Toxicol., 5 (1992) 302–309.
[37] C.A. Angell and E.J. Sare, J. Chem. Phys., 52 (1970) 1058–1068.
[38] H. Jeong, Ph.D. thesis, Iowa State University (1991).
[39] D. Haarer, J. Chem. Phys., 67 (1977) 4076–4085.
[40] J.M. Sayer, A. Chadha, S.K. Agarwal, H.J.C. Yeh, H. Yagi and D.M.Jerina, J. Org. Chem., 56 (1991) 20–29.
[41] H. Rodriguez and E.L. Loechler, Carcinogenesis, 14 (1993) 373–383.
[42] H. Rodriguez and E.L. Loechler, Biochemistry, 32 (1993) 1759–1769.